Research Square

Preprints are preliminary reports that have not undergone peer review.
They should not be considered conclusive, used to inform clinical practice,
or referenced by the media as validated information.

Prediction Models for Energy Consumption and Surface Quality in Stainless Steel Milling

Shuo Yu
Shandong University of Technology
Guoyong Zhao (zgy709@126.com)
Shandong University of Technology
Chunxiao Li
Shandong University of Technology
Shuang Xu
Shandong University of Technology
Zhifu Zheng
Shandong University of Technology

Research Article

Keywords: stainless steel, specific energy consumption, surface roughness, hardness, tool wear

Posted Date: April 12th, 2021

DOI: https://doi.org/10.21203/rs.3.rs-395509/v1

License: This work is licensed under a Creative Commons Attribution 4.0 International License.
Read Full License

Prediction Models for Energy Consumption and Surface Quality in Stainless Steel Milling

Shuo Yu[1] · Guoyong Zhao[1*] · Chunxiao Li[1] · Shuang Xu[1] · Zhifu Zheng[1]

Abstract
Stainless steel is a kind of difficult-to-machine material, and the work hardening in milling easily leads to high energy consumption and poor surface quality. Thus, the influence of machined surface hardness on energy consumption and surface quality cannot be ignored. To solve this problem, the prediction models for machine tool specific energy consumption and surface roughness are developed with tool wear and machined surface hardness considered firstly. Then, the validity of the models is verified through AISI 304 stainless steel milling experiments. The results show that the prediction accuracy of the machine tool specific energy consumption model can reach 98.7%, and the roughness model can reach 96.8%. Later, according to the developed prediction models, the influence of milling parameters, surface hardness, and tool wear on the machine specific energy consumption and surface roughness is studied. Results show that in stainless steel milling, the most significant parameters for surface roughness is the machined surface hardness, while that for energy consumption is the feed per tooth. The machine specific energy consumption increases linearly with the increase of the tool wear and the machined surface hardness gradually. The proposed models are helpful to optimize the process parameters for high efficiency and high quality machining of stainless steel.

Keywords stainless steel · specific energy consumption · surface roughness · hardness · tool wear

1 Introduction

The manufacturing industry plays an important role in economic globalization and sustainable development, which has become the main cause of global warming due to the excessive consumption of energy and the large amount of greenhouse gas emissions in processing [1]. In addition, CNC machining technology has been widely used in manufacturing industry with low processing efficiency, energy consumption and other problems exposed, which makes green and efficient manufacturing become the goal pursued by modern enterprises. Therefore, the research on energy consumption of machine tools and surface quality of parts is more important. For the manufacturing industry, in the case of existing machining equipment, how to reduce energy consumption while improve the surface quality of machining to achieve green energy efficient manufacturing is a critical issue [2].

Specific energy consumption (SEC) is a key evaluation standard for machine efficiency and energy consumption. At present, both foreign and domestic scholars have made in-depth studies on the energy consumption of machine tools. The study on energy consumption prediction models is composed of two main aspects: direct models and indirect models. For direct models, cutting

* Corresponding author
Guoyong Zhao
zgy709@126.com
[1] Institute for Advanced Manufacturing, Shandong University of Technology, Zibo 255000, China

parameters, material removal rate (MRR) and tool wear are mainly used as inputs, and cutting energy or specific energy as outputs to develop a mathematical model to quantitate the cutting energy consumption of machines. For example, Kara and Li [3] developed a relationship model between SEC and MRR, which made more accurate assessment of energy consumption in actual production. Li, Yan and Xing [4] presented a SEC model in relation to MRR and spindle speed, which was tested by medium-carbon steel milling experiments. Zhang et al. [5] developed an exponential model of SEC and cutting parameters according to cutting force empirical formula, and analyzed the influence on parameters in detail. Li et al. [6] optimized the relationship model between specific energy and process parameters to derive the optimal combination of cutting parameters for energy efficient milling. Liu et al. [7] developed a mathematical model at the machine tool, spindle and process aspects to study the influence of cutting parameters on SEC at different stages in milling.

Though these models can accurately predict energy consumption, they fail to consider the influence of factors other than cutting parameters on energy consumption, such as tool parameters or tool wear. Based on this consideration, Zhao et al. [8] analyzed the effect of tool wear on machine tool energy consumption in 45# steel semi-finishing milling, and developed a machine power model with MRR and tool wear as the inputs. The study showed that cutting energy consumption can be reduced by monitoring and controlling tool wear. In a study by Sujan et al [9], Taguchi was used to optimize cutting parameters to reduce the tool wear, it also proved that tool wear can influence energy consumption indirectly. Mativenga and Rajemi [10] developed a carbon emission prediction model, and the model took the tool parameters and cutting parameters as the inputs. Then the cutting parameters were optimized to achieve a balance between minimum energy consumption and minimum processing time, which concluded that the increase of spindle speed and feed rate can improve machining efficiency, reduce energy consumption and rate of tool wear.

For indirect models, the available studies generally use gray correlation theory, neural networks, response surface methods (RSM) and so on to predict machine energy consumption by training and finding the optimal parameters. For instance, Al-Hazza, et al. [11] studied the energy consumption variation regularity under different cutting speeds, feed rates and amount of cutting depth through AISI 4340 steel cutting experiments, BP neural network was used to train the experimental data, and RSM was used to establish a prediction model of machine tool energy consumption and cutting power. Quintana, Ciurana and Ribatallada [12] analyzed the electrical energy consumption of AISI H13 steel in high-speed milling, used artificial neural network to build a prediction model for electrical energy consumption, and investigated the influence of process parameters on electrical energy consumption. Carmita [13] used the RSM algorithm to develop and optimize prediction models for energy consumption and surface quality with cutting parameters and MRR as inputs, which was verified through the AISI 6061 T6 aluminum alloy turning experiment, then they compared the results with empirical parameters experiment results, which showed that energy consumption was significantly reduced after optimization. Hanafi, Khamlichi and Cabrera [14] studied the influence of cutting parameters on energy consumption and surface quality through PEEK-30 dry-turning experiments, optimized the multi-objective model by gray correlation theory, and concluded that cutting depth and cutting speed have significant effects on energy consumption and surface roughness.

Surface quality is a comprehensive standard for evaluating the working performance of parts. The surface roughness, as one of the important indicators of surface quality, has significant impact on the service life and reliability of mechanical products [15]. In recent years, the factors affecting surface roughness in turning and milling has been widely studied, and tool wear, cutting forces are

gradually taken into account in surface roughness prediction models. Asit and Kalipada [16] used RSM to develop a surface roughness model for machined surfaces, with cutting parameters and ambient temperature as the inputs and ultimately found a combination of cutting parameters which can reduce tool wear to a certain extent and obtain the best surface quality. Liu et al. [17] predicted surface roughness in slot milling through three models which are exponential model, linear model and power function model, and the results showed that the power function model could more accurately predict the relationship between surface roughness and cutting parameters. Wang et al. [18] developed a milling surface roughness prediction model considering mechanical factors, tool parameters, cutting parameters and microhardness, and obtained the optimum milling parameters by analyzing the influence of parameters on surface roughness through Ti6AL4V milling experiment.

On the basis of roughness prediction models, some scholars have made multi-objective optimization of surface quality and energy consumption in relation to energy consumption, for instance, Kummer [19] selected C360 copper alloy material to perform micro-turning experiments, used genetic algorithm to optimize multi-objective model based on the best surface roughness and the maximum material removal rate and ultimately obtained the best cutting parameters as spindle speed n =1686r/min, feed rate v_f=10.62μm/r, and cutting depth a_p=99.45μm. Kant and Sangwan [20] proposed a multi-objective prediction model based on minimum energy consumption and optimal surface roughness, the gray correlation and RSM were used to analyze and optimize the model, and the results showed that the feed rate is the most important parameter affecting the multi-objective model. Li et al. [21] developed a third-order polynomial prediction model of cutting force and surface roughness, and optimized the multi-objectve model of cutting force, surface roughness and MRR based on RSM and ITLBO algorithm. The Optimized cutting parameters can get better processing quality tested by 7050 aluminum alloy milling experiment. Although existing studies have considered the influence of the tool, workpiece, and cutting force on the surface roughness, they fail to consider the changes of the surface hardness during the machining process. Actually, in hard-to-cut materials processing, due to the high hardness of the material, large amount of cutting heat is generated in cutting, which increases the temperature of the shear surface obviously and causes serious hardening of the material surface. The increase of the tool-chip contact area makes the friction between the machined surface and the cutter surface increase, which affected the machined surface quality and cutting energy consumption [22].

Presently, the problem of energy consumption and surface quality prediction in hard-to-cut material processing has not been solved yet. To address this problem, the article conducted the following three studies: (1) to develop a *MSEC* prediction model with surface hardness and tool wear considered based on machine energy consumption characteristics. (2) to develop a surface roughness prediction model based on cutting parameters and hardness. (3) to analyze the influence of cutting parameters, tool wear and surface hardness on *MSEC* and surface roughness prediction model.

2. Prediction of Machine tool specific energy consumption

2.1. energy consumption analysis in CNC milling

The CNC milling process has multiple energy consumption parts, complex regularities, and enormous energy consumption. Fig. 1 shows the energy conversion process of machining a blank into a product with specific appearance characteristics.

Fig. 1 Energy conversion in CNC milling.

Existing energy consumption models for CNC machine tools usually reflects relationship between power and machining time. In terms of the composition of energy consumption, the energy consumption of CNC systems can be divided into two categories. One is only related to the characteristics of the specific machine tool itself, mainly including standby energy consumption $E_{standby}$, main drive system and feed system no-load energy consumption $E_{no\text{-}load}$. The other is load-related energy consumption, which is related to the process parameters, workpiece and tool parameters of the machining process, including cutting energy $E_{cutting}$, additional load energy $E_{cutting}$ and processing-related energy consumption of auxiliary systems $E_{auxiliary}$. Since the measurements of $E_{cutting}$ and $E_{auxiliary}$ are very small, the article does not take them into account. In order to establish an energy consumption model to quantitatively calculate the consumption of the CNC milling, it is necessary to analyze the time period characteristics of the processing in conjunction with the consumption unit of the CNC system to determine the consumption state of each time period, as shown in Fig.2.

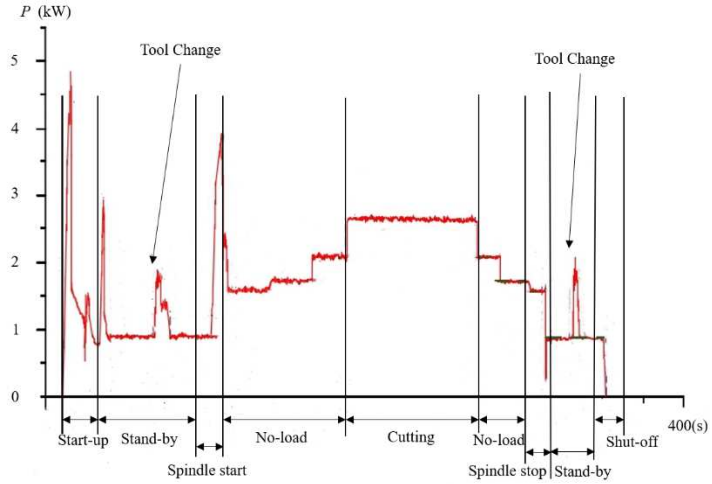

Fig. 2 Power time period characteristics in milling

The article analyzes the energy consumption of VMC850 CNC machining center in combination with characteristics of the time period of CNC milling as follows:

(1) Standby stage energy consumption

During the machine standby stage, which is the period between machine start-up and spindle operation. Energy consumption components include the machine control unit, lighting system, cool system and other auxiliary systems. The power of the machine at this period is the standby power $P_{standby}$, the value of which is considered a constant [4]. According to the preliminary test, the system power of machine tools in different states during the standby period is checked separately, and the results are shown in Table 1. The lighting system and other auxiliary systems consume less power,

which can be neglected in actual calculation. Then the machine tool energy consumption in standby stage E_{standby} is:

$$E_{standby} = P_{standby} \cdot t_{standby} = (P_{control} + P_{cooling} + P_{light}) \cdot t_{standby} \quad (1)$$

Where t_{standby} is machine standby stage time in s, P_{control} is control unit power, P_{cooling} is cool system power, and P_{light} is lighting system power in W.

Table 1 Results of standby power

Condition	Power(W)	System	Power(W)
Light off, Cool off	385.47	P_{control}	385.47
Light on, Cool off	402.89	P_{cooling}	307.26
Light off, Cool on	696.10	P_{light}	14.04
Light on, Cool on	710.1467	P_{standby}	710.1467

(2) No-load energy consumption

The period when the spindle is working but the tool is not touching the workpiece is air-cutting stage, and the power consumed by machine tool at this stage is main drive system and feed system no-load power $P_{\text{no-load}}$. According to the previous test, the spindle speed is set in the range of 200r/min~2500r/min, and the power measurement result is collected once for every 100r/min increase, the results are shown in Table 2.

Table 2 Results of spindle no-load power

n (r/min)	200	300	400	500	600	700	800	900
$P_{\text{no-load}}$ (W)	610.61	632.62	653.19	672.50	692.67	715.10	736.18	757.29
n (r/min)	1000	1100	1200	1300	1400	1500	1600	1700
$P_{\text{no-load}}$ (W)	842.27	863.06	882.40	904.86	924.42	945.00	963.53	980.60
n (r/min)	1800	1900	2000	2100	2200	2300	2400	2500
$P_{\text{no-load}}$ (W)	913.93	884.51	861.56	846.00	834.85	829.93	826.12	821.60

Based on the measurement results, the relationship between no-load power and spindle speed is approximately within the segmented function, as shown in Fig. 3. Then the machine tool no-load energy consumption $E_{\text{no-load}}$ is:

$$\begin{aligned} E_{no-load} &= P_{no-load} \cdot t_{air-cutting} \\ &= \begin{cases} 0.25n + 550.46, & n \in [200,\ 1000) \\ 0.20n + 645.9, & n \in [1100,\ 1800) \\ -2.27 \times 10^{-4} n^2 - 1.09n + 2155, & n \in [1800,\ 2500] \end{cases} \times t_{air-cutting} \end{aligned} \quad (2)$$

Where $t_{\text{air-cutting}}$ is the time of machine air-cutting stage in s, n is spindle speed in r/min.

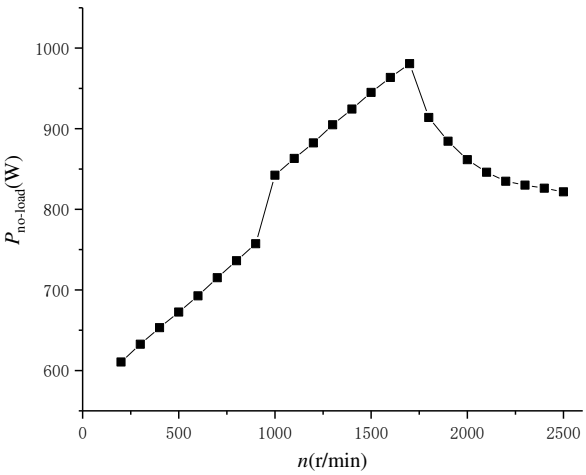

Fig. 3 No-load power of spindle relation curve

(3) Cutting consumption

The cutting stage is the period from the time when the tool touches the workpiece until it leaves after cutting, and the power consumed by the machine during this period is cutting power $P_{cutting}$, including $P_{spindle}$, $P_{feeding}$, $P_{standby}$ and $P_{no\text{-}load}$. Since $P_{feeding}$ is small and can be neglected in calculation, and the power of the cutting stage $P_{cutting}$ can be directly measured. Then cutting consumption $E_{cutting}$ is:

$$E_{cutting} = P_{cutting} \cdot t_{cutting} \tag{3}$$

Where $t_{cutting}$ is cutting stage time in s.

2.2. A Machine tool specific energy consumption (MSEC) model based on hardness and tool wear

Use the specific energy consumption *SEC* (J/mm^3) to evaluate the energy efficiency of the machine tool, which is calculated as the ratio of the total energy consumption E_{total} (J) to the material removal volume *MRV* (mm^3) in milling by Eq. (4). Select the milling depth a_p (mm), milling width a_e (mm), feed per tooth f_z (mm/z), milling speed v_c (m/min), tool flank wear *VB* (mm), and machined surface hardness *H* (N/mm^2) as the inputs to develop the machine specific energy consumption model (*MSEC*). Based on the previous analysis, the *MSEC* model is developed in two parts: the fixed energy consumption (*FEC)* and variable energy consumption (*VEC*), similar to the exponential relationship between the turning parameters and the specific energy consumption, an exponential model is used to establish the *TSEC* as shown in Eq. (6), Eq. (7) and Eq. (8).

$$SEC = \frac{E_{total}}{MRV} = \frac{P_{total} \cdot t}{MRR \cdot t} = \frac{P_{total}}{a_p \cdot a_e \cdot v_f} \tag{4}$$

Where v_f is federate in mm/min, the relational between v_f and f_z is shown in Eq (5).

$$\begin{aligned} v_f &= Z \cdot n \cdot f_z \\ &= Z \cdot \frac{1000 \times v_c}{\pi \times d} \cdot f_z \end{aligned} \tag{5}$$

Where *Z* is milling tool teeth number, *Z*=2, *d* is milling tool shank diameter, *d*=25mm.

$$\begin{aligned} FEC &= \frac{E_{standby}}{MRV} \\ &= \frac{t_{standby} \cdot \left(P_{control} + P_{cooling}\right)}{t_{standby} \cdot MRR} \\ &= \frac{706}{a_p \cdot a_e \cdot v_f} \end{aligned} \tag{6}$$

$$VEC = A \cdot a_p^b \cdot a_e^c \cdot {f_z}^d \cdot v_c^e \cdot (1 + VB)^m \cdot H^n \tag{7}$$

$$\begin{aligned} MSEC &= FEC + VEC \\ &= \frac{706}{a_p \cdot a_e \cdot v_f} + A \cdot a_p^b \cdot a_e^c \cdot {f_z}^d \cdot v_c^e \cdot (1 + VB)^m \cdot H^n \\ &= \frac{K}{a_p \cdot a_e \cdot v_c \cdot f_z} + A \cdot a_p^b \cdot a_e^c \cdot {f_z}^d \cdot v_c^e \cdot (1 + VB)^m \cdot H^n \end{aligned} \tag{8}$$

Where A, K, b, c, d, e, m and n is coefficients to be determined.

3. Stainless steel milling experiments

3.1. Orthogonal experimental design

The orthogonal experiment was designed by Taguchi method, and the four parameters of milling (a_p, a_e, v_c and f_z) were chosen as controllable factors. The range of parameters is a_p = (0.2~0.14) mm, a_e = (2~15) mm, v_c= (66~150) m/min, f_z= (0.1~0.25) mm/z, which is determined by the cutting capacity principle of the carbide milling tool in stainless steel processing. According to the parameter range, the orthogonal experiments with 25 groups of 4 factors and 5 levels were designed as shown in Table 3.

Table 3 Processing parameters level

Factor level	Milling depth a_p/(mm)	Milling side depth a_e/(mm)	Cutting speed v_c/(m/min)	Feed per tooth f_z/(mm/z)
1	0.2	4.0	75	0.12
2	0.5	5.5	90	0.15
3	0.8	7	105	0.18
4	1.1	8.5	120	0.21
5	1.4	10	135	0.24

3.2. Experimental Equipment and Data Collections

The hard-to-cut material AISI 304 stainless steel was used to perform plane wet milling experiments, and the workpiece dimensions are 50mm(length) × 50mm(width) × 30mm(height). Considering the difficulty of hard-to-cut processing, down milling was selected in processing in experiment as shown in Fig. 4 which can slow down the tool wear and improve the surface quality to some extent. Before the experiment, pre-milling of the upper surface of the workpiece of 1 mm depth was carried out to remove the rusted and hardened surface layer to reduce experimental errors due to surface inhomogeneity.

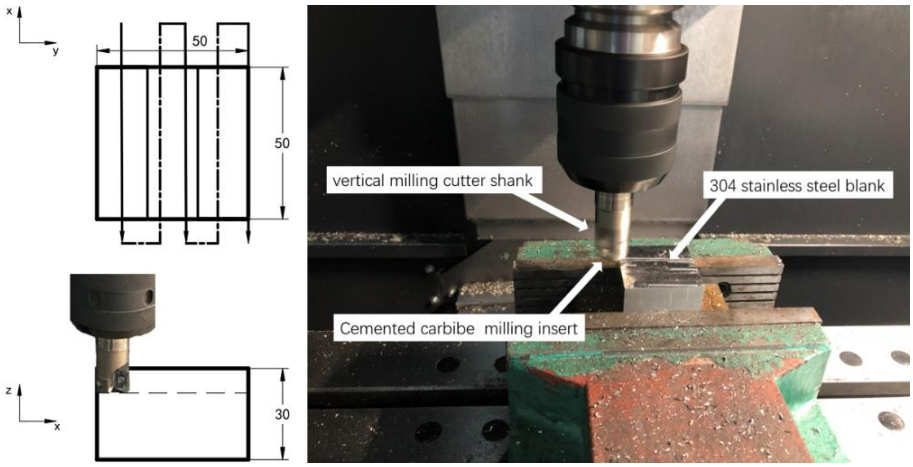

Fig. 4 Diagram processing of milling

The processing equipment is VMC850 CNC machining center (SHENYANG Machine Tool, SMTCL). The cutting tool is a 25mm diameter right-angle and rotatable-position mill cutter (TAP400R-2525-160) with two KYOCERA carbide inserts (APMT1604PDER-KZ), specific parameters as shown in Table 4.

Table 4 Machine tool and tool parameters

Machine tool model	Spindle power P_i/kW	Spindle speed range n/(r/min)	Feed speed range f/(mm/min)	Maximum tool diameter d_{max}/mm	Cooling motor power P_l/W
VMC850E	7.5	50~8000	1-10000	80	460

Tool type	front angel	back angel	Cutting edge angle	Tip permissible error	shank diameter
Carbide	11°	15°	90°	±0.08mm~±0.18mm	25 mm

The measurement instruments required for the experiment are shown in Fig.5. The power and energy signals during the milling process of CNC machine center are collected by a power analyzer (Yokogawa WT500), and the data are processed by WTVIEWEREFREE software, which can calculate the *SEC* indirectly through Eq. (9).

$$\begin{aligned} SEC &= \frac{WP\Sigma \cdot 3600}{MRV} \\ &= \frac{\left[\frac{1}{N}\sum_{n=1}^{N}\{u(n)\cdot i(n)\}\right]\cdot T\cdot 3600}{MRR\cdot t} \\ &= \frac{\left[\frac{1}{N}\sum_{n=1}^{N}\{u(n)\cdot i(n)\}\right]\cdot T\cdot 3600}{\frac{a_p\cdot a_e\cdot v_f}{60}\cdot t} \end{aligned} \tag{9}$$

Where $WP_{\sum}$ is the sum of positive and negative active power for each data update cycle collected by the power analyzer in W·h, N is the sample count of the integration time, $u(n)$ and $i(n)$ are the nth voltage and current measurements, T is the total time of the sampling process in h.

Table 5 Orthogonal experimental table and test results

Test number	a_p (mm)	a_e (mm)	v_c (m/min)	f_z (mm/z)	*VB* (mm)	*H* (N/mm^2)	*Ra* (um)	*MSEC* (J/mm^3)
1	0.2	4	75	0.12	0.070	405	0.389	391.019
2	0.2	5.5	90	0.15	0.089	426	0.797	197.311
3	0.2	7	105	0.18	0.100	394	0.378	114.850
4	0.2	8.5	120	0.21	0.112	402	0.426	74.702
5	0.2	10	135	0.24	0.122	381	0.509	51.777
6	0.5	4	105	0.15	0.138	440	0.794	97.574
7	0.5	5.5	120	0.18	0.154	456	0.758	55.907
8	0.5	7	135	0.21	0.096	458	0.747	33.922
9	0.5	8.5	75	0.24	0.108	438	0.37	38.897
10	0.5	10	90	0.12	0.132	426	0.398	55.775
11	0.8	4	135	0.18	0.141	410	0.784	43.306
12	0.8	5.5	75	0.21	0.155	419	0.534	42.856
13	0.8	7	90	0.24	0.165	407	0.571	26.151
14	0.8	8.5	105	0.12	0.172	403	0.414	37.454
15	0.8	10	120	0.15	0.184	394	0.444	23.648
16	1.1	4	90	0.21	0.194	432	1.095	36.767
17	1.1	5.5	105	0.24	0.089	436	0.874	21.438
18	1.1	7	120	0.12	0.121	426	0.601	30.338
19	1.1	8.5	135	0.15	0.142	420	0.587	20.256
20	1.1	10	75	0.18	0.085	435	0.765	20.549
21	1.4	4	120	0.24	0.114	442	0.558	21.469
22	1.4	5.5	135	0.12	0.074	433	0.373	27.829
23	1.4	7	75	0.15	0.103	428	0.881	28.595
24	1.4	8.5	90	0.18	0.110	425	0.572	18.714
25	1.4	10	105	0.21	0.130	432	0.719	12.252

A roughness tester (RTP120) was used to measure the machined surface roughness (*Ra*) of the workpiece, and 5 points evenly distributed on the workpiece surface were selected for measurement to average, which can obtain statistically significant *Ra* values. A microscope (ZEISS Axio Lab.A1 Mat) was used to measure *VB* values, and the average of the two measurements before and after the experiment was taken as the values of *VB* for this group experiments, and replace the inserts in the event of tool wear up to 0.2mm. Since the frequent removing and resetting of workpieces in continuous milling would cause discontinuous data on *SEC*, *VB*, and *Ra*, and could not reflect the effect of changing cutting parameters on energy consumption and surface quality, thus, a Leeb hardness tester was chosen to measure the hardness values (*H*) of each group of experiments before processing without damaging the surface quality of the workpiece. The orthogonal experimental tables L25(5^4) and data collection results are shown in Table 5.

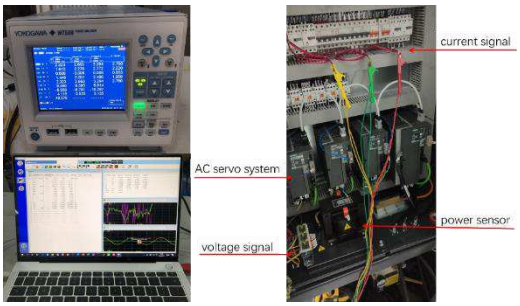

(a) RF power analyzer and signal acquisition

(b) Surface roughness measurements

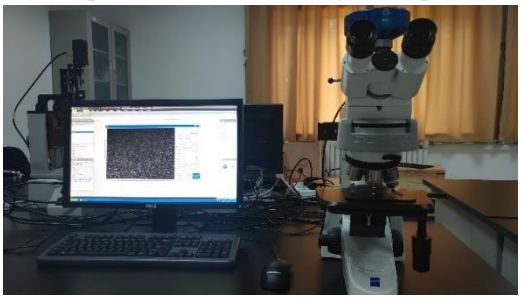

(c) Tool wear measurement system

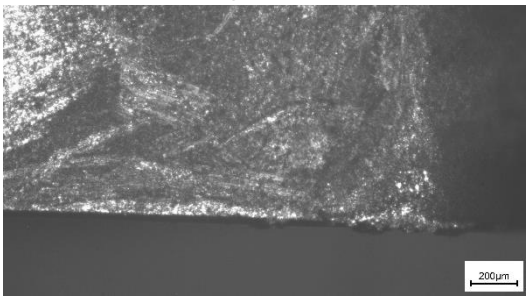

(d) Tool wear measurement result

Fig. 5 Measuring apparatus

4. Machine tool specific energy consumption (*MSEC*) and surface roughness (*Ra*) prediction models

4.1. MSEC model fitting and parametric analysis

The *MSEC* prediction model can be obtained with least square method through nonlinear curve fitting with the 25 sets of data in Table 5 as Eq. (10). The determination coefficient R^2 is widely used to evaluate regression effect in model, and the results show that the R^2 of *MSEC* model was 99.3%, and R^2 (adjusted) reached 98.7%. The error and ANOVA of *MSEC* model are shown in Fig. 6 and Table 6.

$$SEC = \frac{2633}{a_p \cdot a_e \cdot v_c \cdot f_z} + 0.055 \cdot a_p^{-0.720} \cdot a_e^{-0.674} \cdot {f_z}^{-0.723} \cdot v_c^{0.514} \cdot H^{0.357} \cdot (1 + VB)^{0.313} \quad (10)$$

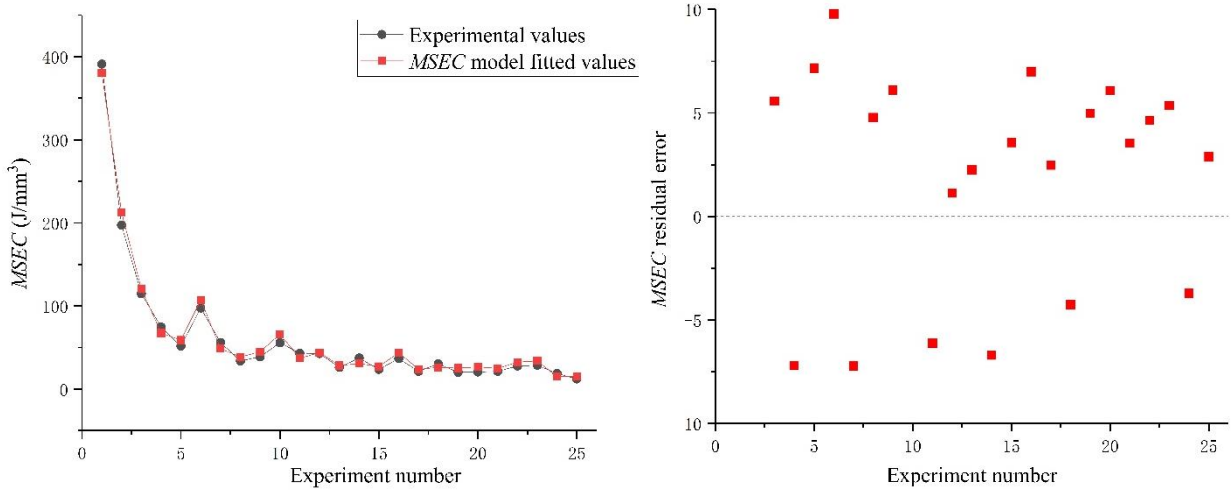

Fig. 6 *MSEC* model fitting results

Table 6 ANOVA for *MSEC* model

	DF	Squares	Mean square error	F
Regression	8	244165	30520	47515
Residual error	17	10.9196	0.6423	
Total	25	244176		

With the identification of setting machining parameters, the pattern of the effects of cutting parameters, tool wear, and hardness of the machined surface on *MSEC* is shown in Fig. 7. In hard-to-cut material milling a_p is the most significant impact followed by a_e and f_z on the machine tool specific energy, which will make the MRR increase and lead to reduce in *MSEC*. The effect of v_c on *MSEC* is not significant in the range of cutting dosage of hard-to-cut materials (90m/min-150m/min), and *MSEC* slowly reduces with the increase of v_c. *MSEC* increases linearly within a certain range with the increase of tool wear and machined surface hardness. Because the workpiece materials components and tool materials reactions under high temperature conditions in hard-to-cut materials cutting, it also leads to the composition separating out of the tool and other phenomena to accelerate tool wear. With the increase of tool wear, the area of the tool and workpiece contact section increases, so that the tip of the tool and the workpiece friction generates more heat in cutting. In addition, due to the low thermal conductivity of most hard-to-cut materials, cutting heat is difficult to diffuse, and the cutting edge is significantly affected by heat, which causes high temperature of cutting edge and leads to increase in surface hardening of the parts, resulting in *MSEC* increasing.

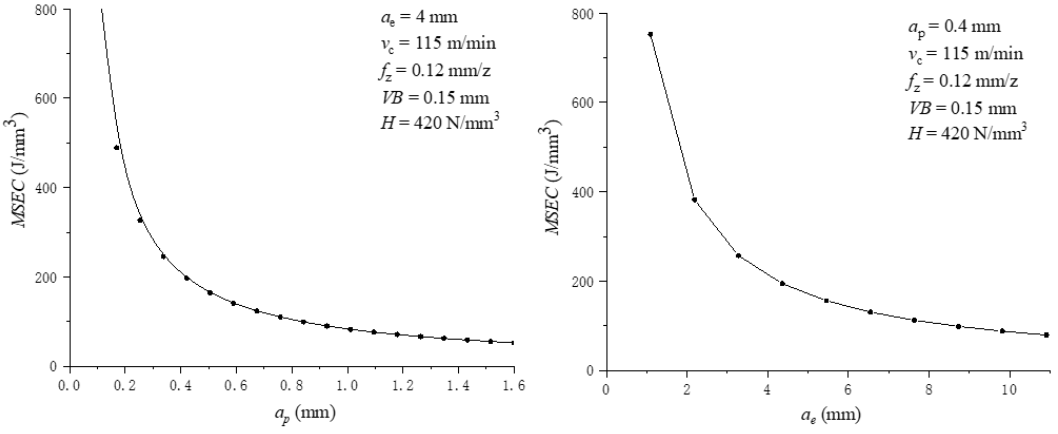

(a) (b)

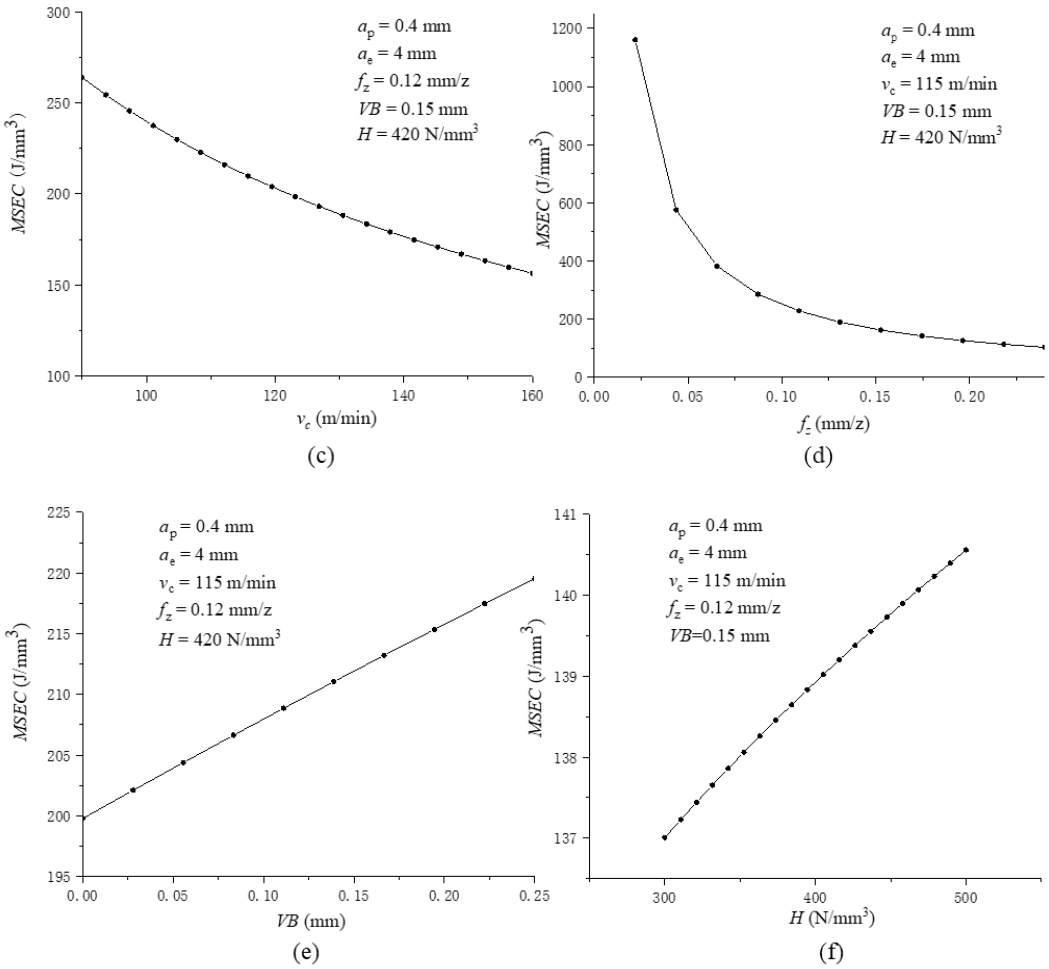

Fig. 7 Influence of machining parameters, tool wear and hardness on *MSEC* model

4.2 Surface roughness prediction model

Surface roughness is an important indicator to measure the surface integrity. There are numerous factors affecting the surface roughness. On the one hand, it is influenced by cutting parameters, tool wear, residual stresses and surface work-hardening during the milling process. On the other hand, the geometry and mechanical properties of the workpiece are also affected the surface roughness, as shown in Fig. 8.

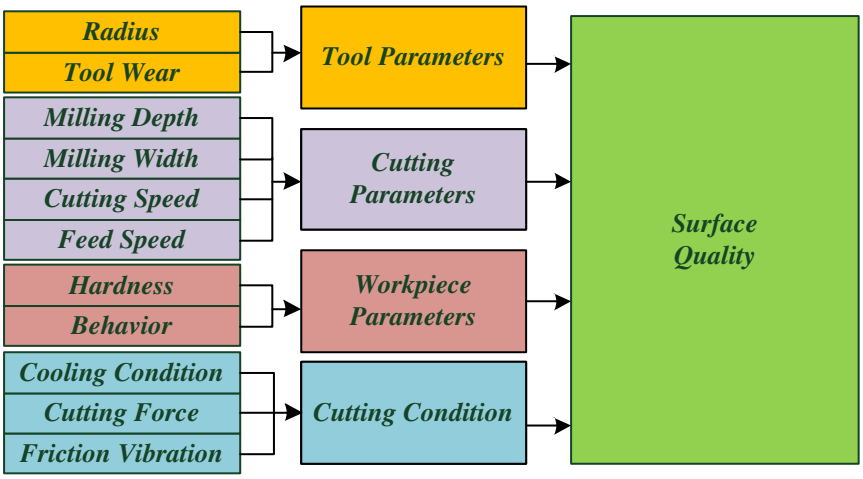

Figure 8. Influence factors of surface quality

Since the relationship between surface roughness and process parameters is not simply linear, thus, the RSM was used to predict the surface roughness and establish a quadratic response surface model for surface roughness, as shown in equation (11).

$$y = \beta_0 + \sum_i \beta_i x_i + \sum_{i<j} \sum_i \beta_{ij} x_i x_j + \sum_i \beta_{ij} x_i^2 + \varepsilon \tag{11}$$

Where y is the response, which indicates the surface roughness in Ra model, x_i is the independent variable, β_i is the coefficient of the regression equation, ε is the error between the fitted and experimental values.

Before response surface analysis, the model variables are linearly transformed to resolve the effects of different ranges and dimensions of the independent variables, and the results are shown in Table 7.

Table 7 Linear transformation results of model variables

RSM variable	Model variable	Linear transformation
A	a_p	A= (a_p -0.8)/0.6
B	a_e	B= (a_e -7)/3
C	v_c	C= (v_c -105)/30
D	f_z	D= (f_z -0.18)/0.06
E	H	E= (H -419.5)/38.5

The milling depth a_p, milling width a_e, cutting speed v_c, feed per tooth f_z and the machined surface hardness H were selected as the inputs, and the surface roughness was used as the response. To verify the effect of machined surface hardness on the model, the regression model Ra_2 considering hardness was compared with the model Ra_1 which only considered four cutting parameters, the fitting results are shown in Eq. (12), Eq. (13) and Fig. 9.

$$Ra1 = 0.658 + 0.085A + 0.151B + 0.023D - 0.075A^2 + 0.053B^2 - 0.05D^2 - 0.084AB - 0.221AC + 0.012BD \tag{12}$$

$$Ra2 = 0.419 - 2.806A - 1.028B - 0.451C + 0.251D + 4.41E - 9.35A^2 - 0.485B^2 + 0.384C^2 - 20.63E^2 - 4.71AB - 1.575AC + 27.83AE - 0.329BD + 7.37BE + 2.83CE \tag{13}$$

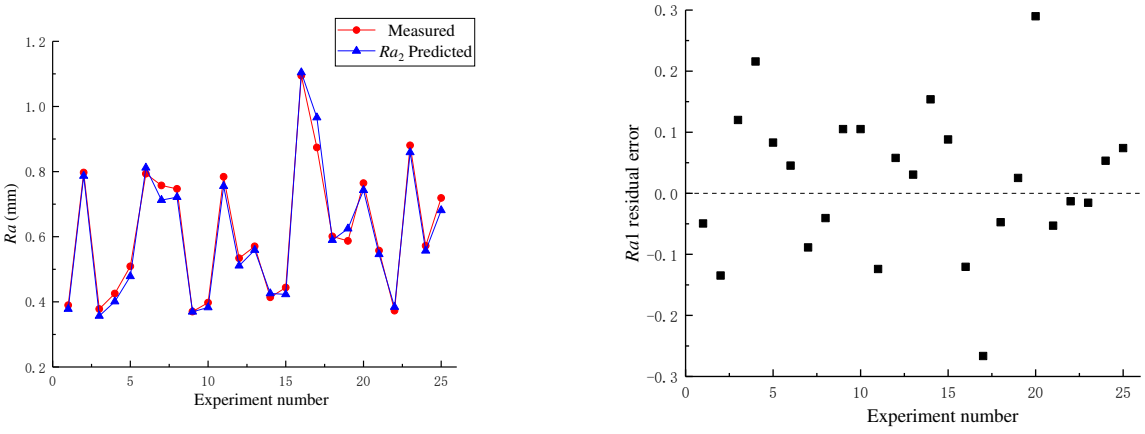

(a) (b)

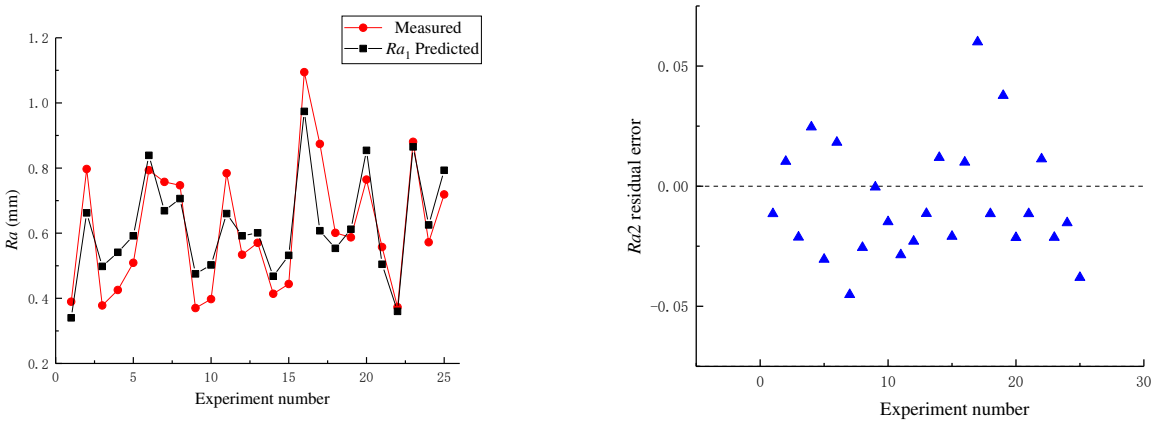

(c) (d)

Fig. 9 Fitting results of roughness prediction model

Significance level was chosen as α=0.05, which meant that the confidence level of the results was above 95%. F-value is the ratio of regression error to mean square error, which was used to measure the significant effect of model terms on response, and the ANOVA results are shown in Table 8 and Table 9. The determination coefficient R^2 was used to assess the fitting of the model, and the results show that the R^2 of the Ra_1 model is 68.5% and the R^2 (adjusted) is 58.7%, the R^2 of the Ra_2 model is 96.7% and the R^2 (adjusted) is 95.8%, which indicated that Ra_2 model considering hardness can predict surface roughness more accurately.

Table 8 Analysis of variance (ANOVA) for Ra_1

Source	DF	Adj SS	Adj MS	F	P
Regression	12	0.620322	0.051693	1.96	0.128
Linear	4	0.287656	0.071914	2.73	0.079
A	1	0.078558	0.078558	2.98	0.110
B	1	0.191783	0.191783	7.28	0.019
D	1	0.004575	0.004575	0.17	0.684
Square	4	0.035673	0.008918	0.34	0.847
*A*A*	1	0.023975	0.023975	0.91	0.359
*B*B*	1	0.008012	0.008012	0.30	0.591
*D*D*	1	0.004157	0.004157	0.16	0.698
Interaction	4	0.152416	0.038104	1.45	0.278
*A*B*	1	0.019094	0.019094	0.73	0.411
*A*C*	1	0.132048	0.132048	5.02	0.045
Residual error	12	0.315926	0.026327		
Total	24	0.936247			

DF：Degree of freedom, SS：Sum of square, MS：Mean square.

Table 9 Analysis of variance (ANOVA) for Ra_2

Source	DF	Adj SS	Adj MS	F	P
Regression	18	0.871460	0.048414	4.48	0.036
Linear	5	0.237845	0.047569	4.41	0.050
A	1	0.153716	0.153716	14.24	0.009
B	1	0.088531	0.088531	8.20	0.029
C	1	0.028857	0.028857	2.67	0.153
D	1	0.002790	0.002790	0.26	0.629
E	1	0.165854	0.165854	15.36	0.008
Square	5	0.238916	0.047783	4.43	0.049
*A*A*	1	0.148865	0.148865	13.79	0.010
*B*B*	1	0.065603	0.065603	6.08	0.049
*C*C*	1	0.097477	0.097477	9.03	0.024
*E*E*	1	0.170406	0.170406	15.78	0.007
Interaction	8	0.382161	0.047770	4.42	0.043
*A*B*	1	0.118863	0.118863	11.01	0.016
*A*C*	1	0.065351	0.065351	6.05	0.049
*A*E*	1	0.160690	0.160690	14.88	0.008
*B*C*	1	0.073724	0.073724	6.83	0.040
*B*E*	1	0.112085	0.112085	10.38	0.018
*C*E*	1	0.037784	0.037784	3.50	0.111
Residual error	6	0.064787	0.010798		
Total	24	0.936247			

4.3 validation of MSEC model and Ra model

Three new combinations of cutting parameters were selected to verify the prediction accuracy of *MSEC* model and *Ra* model, and the results are shown in Table 10 and Table 11. The accuracy of machine tool specific energy prediction results for all three groups of experiments is above 95%, which indicates that the *MSEC* model considering hardness and tool wear has high accuracy. For surface roughness prediction, the accuracy results of Ra_1model are only about 50%, while that of Ra_2 model is above 90%, which obviously shows that the *Ra* model considering the material hardness can predict the surface roughness more accurately in hard-to-cut materials processing.

Table 10 Cutting parameters of test experiments and measurement results

Test number	a_p (mm)	a_e (mm)	v_c (m/min)	f_z (mm/z)	*VB* (mm)	*H* (N/mm^2)	*Ra* (um)	*MSEC* (J/mm^3)
1	0.4	6	100	0.20	0.072	405	0.897	62.497
2	0.6	8	85	0.1	0.085	416	0.576	75.755
3	0.8	4	120	0.18	0.103	424	0.392	46.612

Table 11 Test experiments prediction model results

Test number	*MSEC* prediction	precision	Ra_1 prediction	precision	Ra_2 prediction	precision
1	64.318	97.08%	0.481	53.62%	0.911	98.44%
2	73.493	97.01%	0.513	89.06%	0.595	96.70%
3	47.272	98.58%	0.560	57.14%	0.370	94.39%

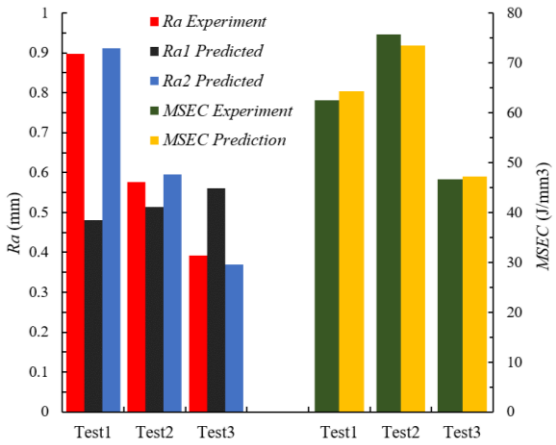

Fig. 10 Comparison of *MSEC* and *Ra* model prediction accuracy

5 Conclusion and future work

Firstly, prediction models for *MSEC* and surface roughness in stainless steel milling were developed respectively. Then the models were verified the reliability through AISI 304 stainless steel milling experiments. At last, the influence of cutting parameters, surface hardness and tool wear on *MSEC* model and *Ra* model was studied. The main conclusions are as follows:

(1) The prediction accuracy of *MSEC* model considering surface hardness and tool wear can reach 98.7%. The model can accurately predict the cutting energy consumption, because in hard-to-cut materials milling, tool wear and surface hardness has significant influence on cutting energy consumption.

(2) The prediction accuracy of Ra_2 model considering hardness can reach 96.8%, which is much greater than that of Ra_1 model considering only cutting parameters, indicating that surface hardness is a nonnegligible factor affecting the machined surface roughness.

(3) The machine specific energy consumption increases linearly with the increase of machined surface hardness, which also leads to an increase in surface roughness. Therefore, in hard-to-cut materials processing, the cutting parameters can be reasonably selected to slow down the hardening, reduce tool wear, decrease cutting energy consumption and improve surface quality.

The future work is as follows:

(1) In order to verify the influence of hardness on surface roughness, tool wear is not considered in the *Ra* model. To develop a more comprehensive surface roughness prediction model combining hardness and tool wear is a problem which needs further study.

(2) The multi-objective optimization of energy consumption and surface quality in hard-to-cut materials processing will be the focus of future study.

Funding information This work was supported by the Key projects of Shandong Province Natural Science Foundation of China [ZR2020KE060].

Data availability All the data have been presented in the manuscript.

Disclosure statement

Conflict of interest The authors declare that they have no known competing financial interests or personal relationships that could have appeared to influence the work reported in this paper.

Code availability Not applicable

References

1. Amy J.C. Trappey, Charles V. Trappey, Chih-Tung Hsiao, Jerry J.R. Ou and Chin-Tsung Chang (2012) System dynamics modelling of product carbon footprint life cycles for collaborative green supply chains. Int J Comput Inter Manuf 25(10): 934-945. https://doi.org/10.1080/0951192X.2011.593304
2. G.Y. Zhao, Z.Y. Liu, Y. He, H.J. Cao and Y.B. Guo (2017) Energy consumption in machining: classification prediction, and reduction strategy. Energy 133: 142-157. https://doi.org/10.1016/j.energy.2017.05.110
3. S. Kara and W. Li (2011) Unit process energy consumption models for material removal processes. CIRP Ann-manuf Techn 60(1): 37-40. https://doi.org/10.1016/j.cirp.2011.03.018
4. L. Li, J.H. Yan and Z.W. Xing (2013) Energy requirements evaluation of milling machines based on thermal equilibrium and empirical modeling. J Clean Prod 52:113-121. https://doi.org/10.1016/j.jclepro.2013.02.039
5. H.C. Zhang, L.L. Kong, T. Li and J.C. Chen (2015) SCE modeling and influencing trend analysis of cutting parameters. China Mech Eng 26(08): 1098-1104. https://doi.org/10.3969/j.issn.1004-132X.2015.08.019
6. C.B. Li, Q.E. Xiao, L. Li and X.F. Zhang (2015) Optimization method of NC milling parameters for energy efficiency based on Taguchi and RSM. Comput. Integr Manuf Syst 21(12): 3182-3191. https://doi.org/10.13196/j.cims.2015.12.010
7. N. Liu, S. B. Wang, Y.F. Zhang and W.F. Lu (2016) A novel approach to predicting surface roughness based on specific cutting energy consumption when slot milling Al-7075. Int J Mech Sci 118: 13-20. https://doi.org/10.1016/j.ijmecsci.2016.09.002
8. G.Y. Zhao, Y. Su, G.M. Zheng, Y.G. Zhao and C.X. Li (2020) Tool tip cutting specific energy prediction model and the influence of machining parameters and tool wear in milling. P. I. Mech. Eng. B-J. Eng. 234 (10): 1346-1354. https://doi.org/10.1177/0954405420911298
9. Sujan Debnath, Moola Mohan Reddy, Qua Sok Yi (2016) Influence of cutting fluid conditions and cutting parameters on surface roughness and tool wear in turning process using Taguchi method. Measurement 78: 111-119. https://doi.org/10.1016/j.measurement.2015.09.011
10. P.T. Mativenga and M.F. Rajemi (2011) Calculation of optimum cutting parameters based on minimum energy footprint. CIRP Ann-manuf. Techn. 60 (1): 149-152. https://doi.org/10.1016/j.cirp.2011.03.088
11. Muataz Hazza Faizi Al-Hazza, Erry Yulian T Adesta, Afifah Mohd Ali, Delvis Agusman and Mohammad Yuhan Suprianto (2011) Energy cost modeling for high speed hard turning. J Appl Sci 11: 2578-2584. https://doi.org/10.3923/jas.2011.2578.2584
12. G Quintana, J Ciurana and J Ribatallada (2011) Modelling power consumption in ball-end milling operations.

Mater Manuf Process 26 (5): 746-756. https://doi.org/10.1080/10426910903536824

13. Carmita Camposeco-Negrete (2015) Optimization of cutting parameters using Response Surface Method for minimizing energy consumption and maximizing cutting quality in turning of AISI 6061 T6 aluminum. J Clean Prod 91: 109-117. https://doi.org/10.1016/j.jclepro.12.017
14. Issam Hanafi, Abdellatif Khamlichi, Francisco Mata Cabrera, Emiliano Almansa and Abdallah Jabbouri (2012) Optimization of cutting conditions for sustainable machining of PEEK-CF30 using TI N tools. J Clean Prod 33 (8): 1-9. https://doi.org/10.1016/j.jclepro.2012.05.005
15. T. Peng and X. Xu (2014) Energy-efficient machining systems: a critical review. Int J Adv Manuf Technol 72: (9-12) 1389-1406. https://doi.org/10.1007/s00170-014-5756-0
16. Asit Kumar Parida, and Kalipada Maity (2019) Modeling of machining parameters affecting flank wear and surface roughness in hot turning of Monel-400 using response surface methodology (RSM). Measurement 137: 375-381. https://doi.org/10.1016/j.measurement.2019.01.070
17. Z.Y. Liu and Y.B. Guo, Sealy M.P and Liu Z.Q (2015) Energy consumption and process sustainability of hard milling with tool wear progression. J Mater Process Tech 229: 305-312. https://doi.org/10.1016/j.jmatprotec.2015.09.032
18. B. Wang, Q. Zhang, M.H. Wang, Y.H. Zheng and X.J. Kong (2020) A predictive model of milling surface roughness. Int J Adv Manuf Technol 108(3): 2755-2762. https://doi.org/10.1007/s00170-020-05599-x
19. S.P. Leo Kumar (2019) Measurement and uncertainty analysis of surface roughness and material removal rate in micro turning operation and process parameters optimization. Measurement 140: 538-547. https://doi.org/10.1016/j.measurement.2019.04.029
20. Girish Kant, and Kuldip Singh Sangwan (2014) Prediction and optimization of machining parameters for minimizing power consumption and surface roughness in machining. J Clean Prod 83: 151-164. https://doi.org/10.1016/j.jclepro.2014.07.073
21. B. Li, X.T. Tian and M. Zhang (2020) Modeling and multi-objective optimization of cutting parameters in the high-speed milling using RSM and improved TLBO algorithm. Int J Adv Manuf Technol 111: 7-8. https://doi.org/10.1007/s00170-020-06284-9
22. L.R. Zhou, F.Y. Li, J.F. Li, C.L. Cheng and L Kong (2018) Milling machine power model considering workpiece material hardness. Comput Integr Manuf 24 (04): 905-916. https://doi.org/10.13196/j.cims.2018.04.010

Figures

Figure 1

Energy conversion in CNC milling

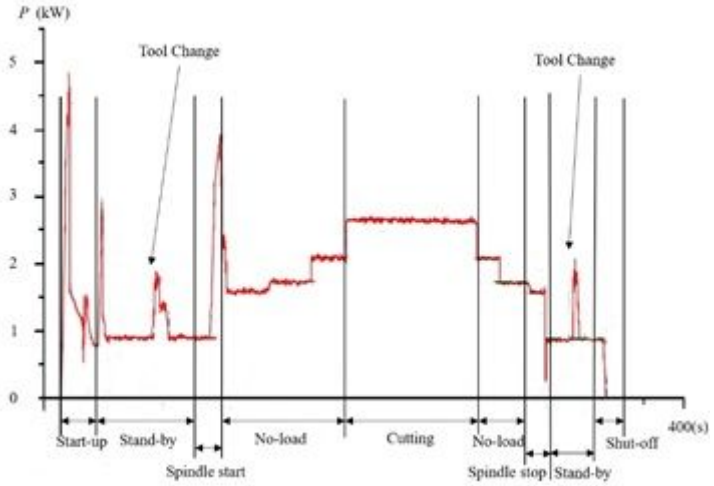

Figure 2

Power time period characteristics in milling

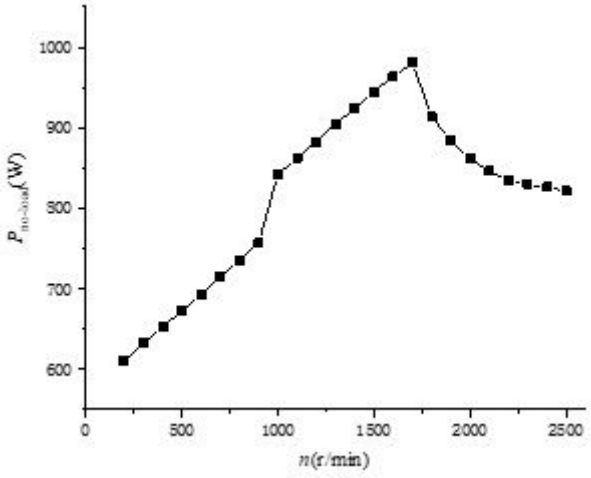

Figure 3

No-load power of spindle relation curve

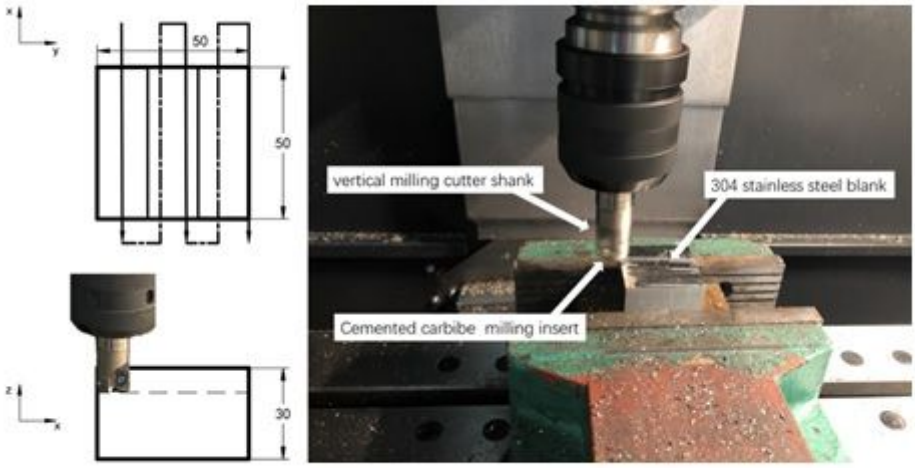

Figure 4

Diagram processing of milling

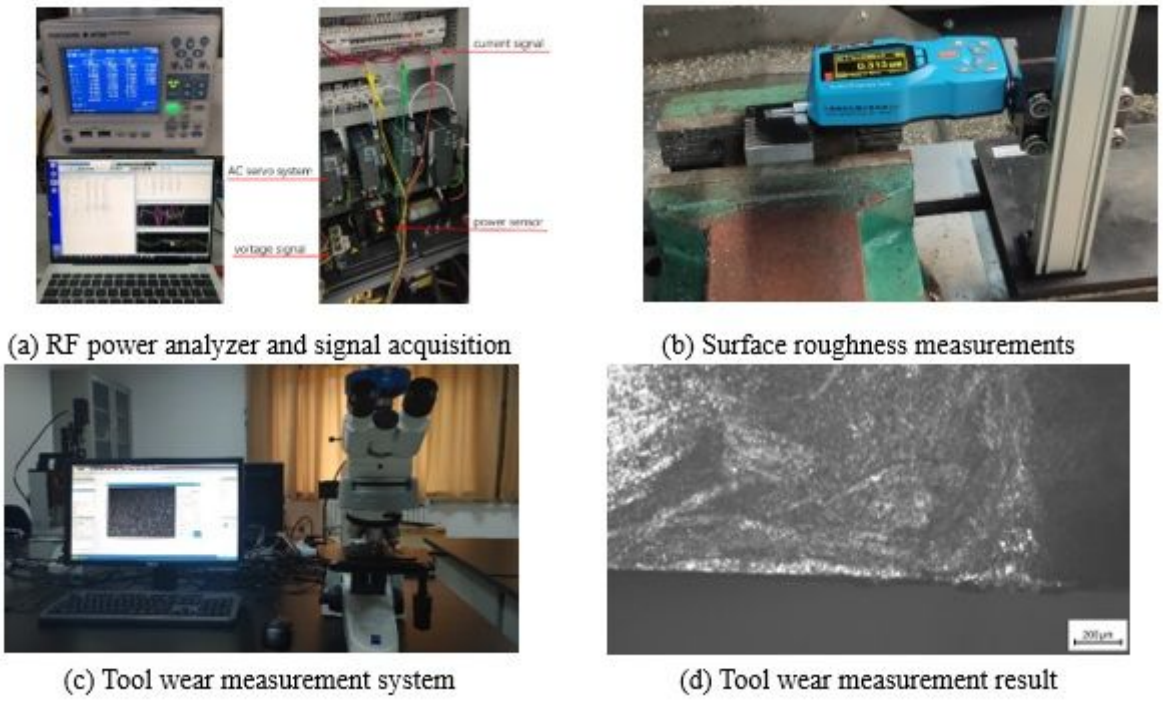

(a) RF power analyzer and signal acquisition

(b) Surface roughness measurements

(c) Tool wear measurement system

(d) Tool wear measurement result

Figure 5

Measuring apparatus

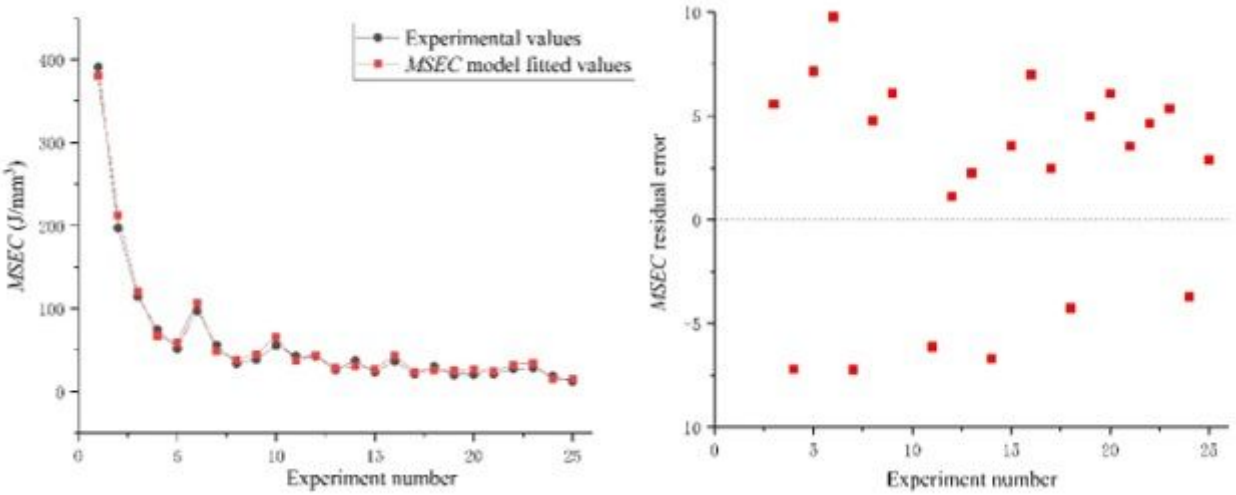

Figure 6

MSEC model fitting results

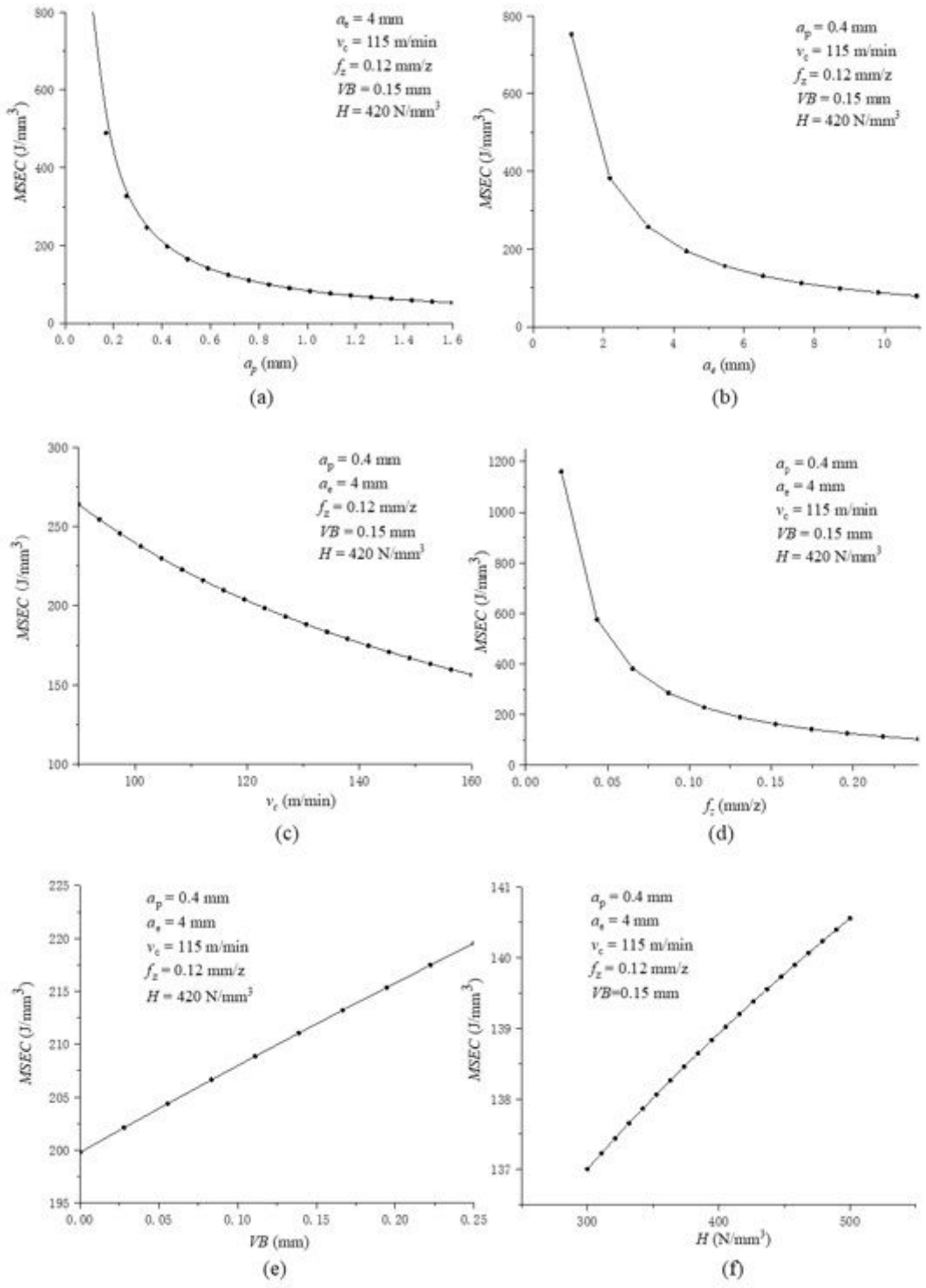

Figure 7

Influence of machining parameters, tool wear and hardness on MSEC model

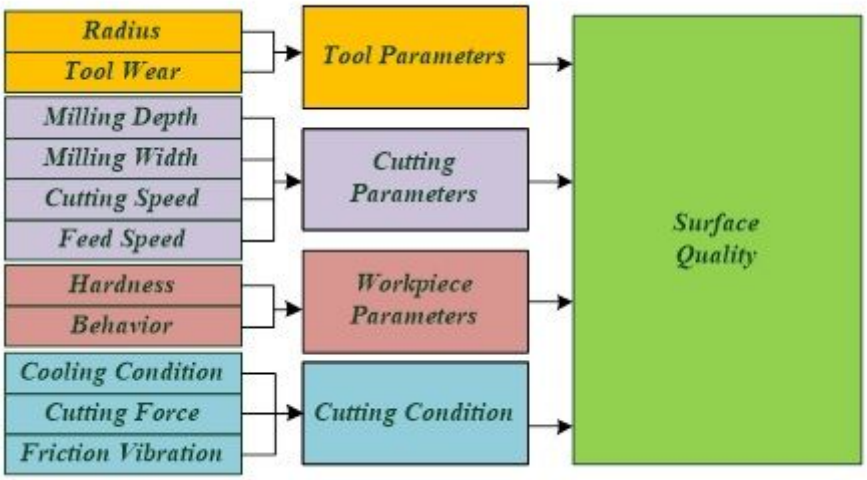

Figure 8

Influence factors of surface quality

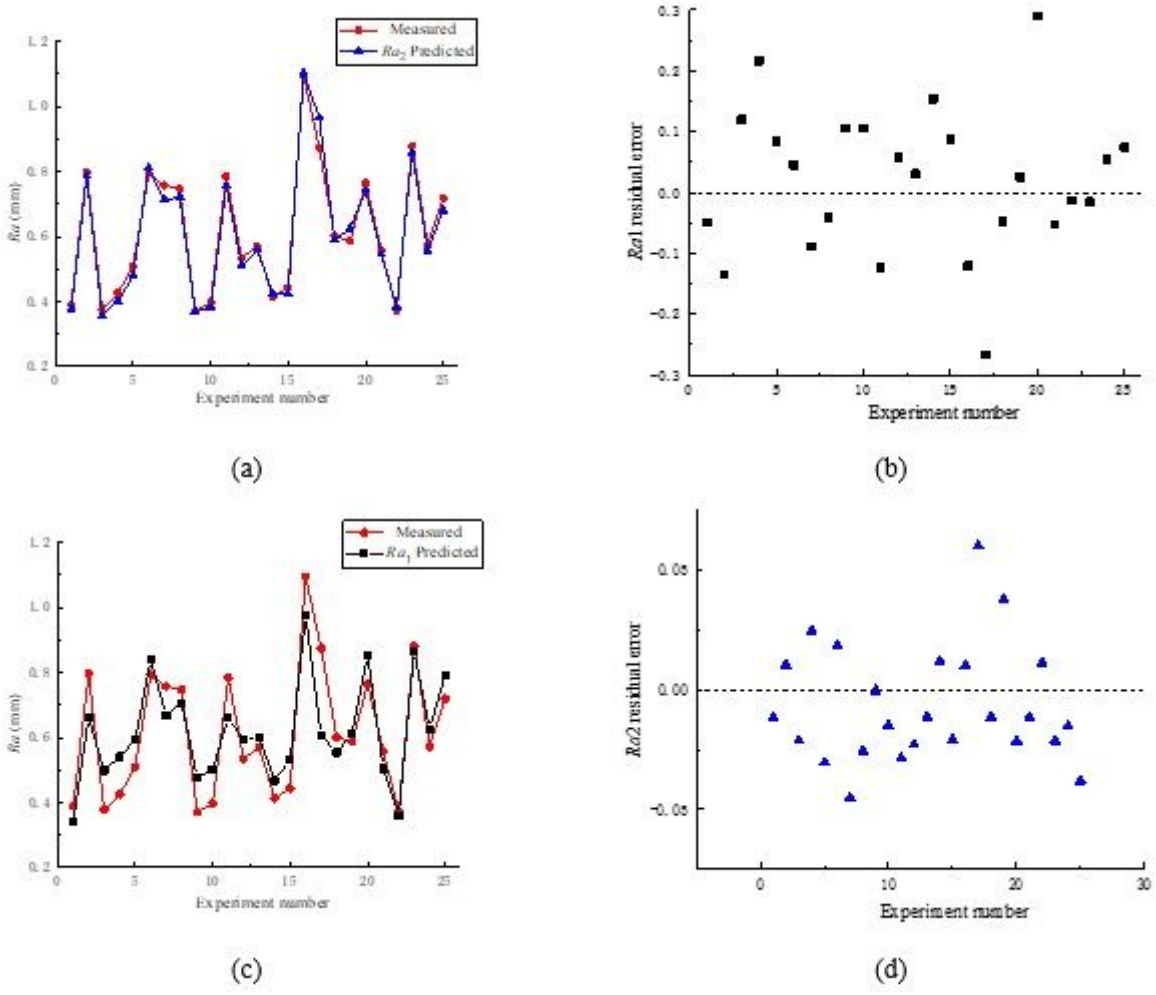

Figure 9

Fitting results of roughness prediction model

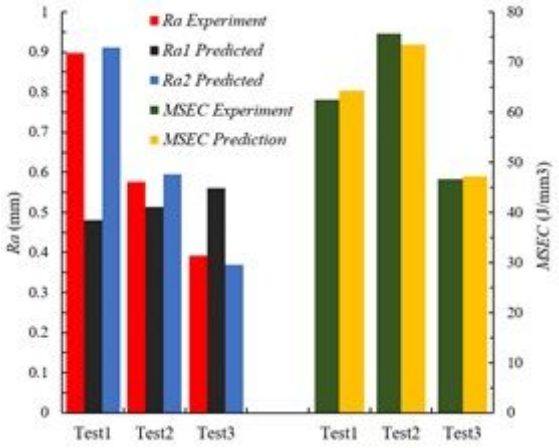

Figure 10

Comparison of MSEC and Ra model prediction accuracy